Bit Error Rate Evaluation of Linear Equalization in FWA Systems

Pei Xiao, Rolando Carrasco
School of Electrical, Electronic and Computer Engineering
University of Newcastle Upon Tyne, NE1 7RU, United Kingdom
E-mail: pei.xiao, r.carrasco@ncl.ac.uk
Ian Wassell
Digital Technology Group, Computer Laboratory, University of Cambridge
15 JJ Thomson Avenue, CB3 0FD, United Kingdom
E-mail: ijw24@eng.cam.ac.uk

Abstract

The bit error rate performance of broadband wireless fixed access (FWA) systems over multipath fading channels is investigated in this paper. Linear MMSE equalization is examined theoretically for 16-QAM and QPSK modulated FWA systems and shown to yield unsatisfactory performance. The theoretical analysis is validated by Monte-Carlo simulations and proved to be reasonably accurate. It provides us an insight into the physical limitations imposed by the FWA channels and suggest solutions to improve the capacity and performance of future FWA systems.

Keywords: broadband fixed wireless access, multipath fading channels, equalization, performance analysis.

I. Introduction

It is becoming apparent that access to the Internet is of growing economic and political importance. It is also clear that low bandwidth dial-up Internet access is restricting the services and applications that can be offered. What is required is a quantum leap in access bandwidth to free up the Internet for innovative applications. One possible solution is to use the existing local-loop. This approach requires the installation of digital subscriber line (DSL) equipment at the exchange and customer premises. Unfortunately, even with advances in DSL technology, the length and quality of the local-loop infrastructure will prevent this service being offered universally. Another option for providing broadband access is via cable TV networks. However, the availability of these services is far from universal. An alternative approach is to deploy broadband fixed wireless access (FWA) technology. The advantage of such an approach is that it enables operators in a competitive environment to roll-out broadband services in a rapid and cost

efficient manner. It is especially suited to the less populated rural areas where a considerable number of households are still beyond the reach of affordable mass-market broadband services, and laying cables and setting up wireline infrastructure are cumbersome and costly. FWA has a significant role to play in order to improve this situation. FWA networks generally employ a point-to-multi-point architecture [1], where a single based station (BS) communicates with many subscriber units (SUs) placed at the user locations. Standardization of FWA systems is currently being undertaken by the IEEE 802.16 working group [2] and the ETSI HIPERMAN group [3].

One of the limiting factors in outdoor wireless transmission is the multipath channel between the transmitter and the receiver giving rise to intersymbol interference (ISI), which degrades the system performance and limits the maximum achievable data rate. The problem can be tackled by employing OFDM technology [4], which transforms the frequency selective channel into a number of parallel flat fading channels. Another effective remedy to combat the detrimental effects caused by ISI is the use of equalization, which is the focus of this study. Various equalization algorithms for the FWA systems have been examined previously, for example, in [5], [6]. The bit error rate (BER) performance is usually measured by simulations in most existing literature (e.g., [5], [6]) for different equalization schemes. Since the evaluation of the exact error probability with ISI is tedious and time-consuming, an upper bound method based on the relationship between the minimum mean square error (MMSE) and the bound of symbol error probability was employed in [7]. The bound is applicable to multilevel as well as binary signals. In [8], a moment method was used to estimate the error rate of a finite-tap equalizer and found to be more accurate than the Chernoff bound. A quasi-analytical moments approach was proposed in [9] to calculate the bit error rate for various infinite-length MMSE equalizers, and shown to offer a substantial performance improvement over the upper bound method. An approximate Fourier series method was applied in [10] to evaluate the performance of finite-length linear equalizer and decision feedback equalizer for QPSK transmission on static and quasi-static Rayleigh fading channels. The approximate Fourier series performs an efficient averaging of the BER across the distribution of the residual ISI. However, to our best knowledge, no results on the performance analysis of equalization for the FWA channels are available in the existing literature. That is previous FWA studies have relied solely on the use of simulation techniques. The FWA channels have either Ricean and Rayleigh distributions for the amplitude of various channel taps, which differentiates them from other channels analyzed in the previous literature. The main contribution of this paper is to provide a theoretical approach to analyze the effect of ISI on the performance of the FWA systems, with an attempt to gain a deep insight into physical limitations imposed by the FWA channels on conventional equalization techniques.

The baseband equivalent of the transmission system under study is shown in Figure 1. The information bits $\{b_n\}$ are first mapped into QPSK/16-QAM symbols $\{s_n\}$, which are subsequently transmitted over the FWA multipath channel. The channel can be modelled by an equivalent baseband system where the concatenation of the the transmit filter, the channel and the receive filter, is represented by a discrete-

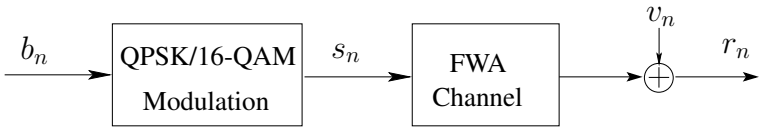

Fig. 1. Block diagram of the FWA transmission system.

time T-tap transversal filter with finite-length impulse response $h_n = \sum_{t=0}^{T-1} h_t \delta_{n-l}$ where h_t denotes the complex channel coefficients. A set of 6 typical statistical channel models called the Stanford University Interim (SUI) Channel Models were proposed in [11] for simulation, design, development and testing of technologies suitable for the FWA applications. All of them are simulated using 3 taps, having either Ricean or Rayleigh amplitude distributions. For the purpose of this study, we select the SUI-3 channel, which fits the terrain conditions of UK rural areas, and also represents a worse case scenario compared to other channel models. This channel model has a tap spacing of 500ns, and maximum tap delay at 1000ns. Under the assumption that the transmitted data rate is 4Mbps with QPSK modulation or 8Mbps with 16-QAM modulation, the multipath fading can be modelled as a tapped-delay line with adjacent taps equally spaced at the symbol rate. The received signal is formed as

$$r_n = h_0 s_n + h_1 s_{n-1} + h_2 s_{n-2} + v_n, \tag{1}$$

where the channel coefficients h_0, h_1, h_2 are complex Gaussian distributed and assumed to remain constant during the transmission of one block of data. They, however, vary from block to block. The amplitude of the first tap $|h_0|$ is characterized by a Ricean distribution due to the presence of line of sight propagation. The amplitudes of the taps $|h_1|, |h_2|$ are Rayleigh distributed. The transmitted PSK/QAM symbol at time instant n is denoted as $s_n = x_n + jy_n$, and v_n is the complex additive white Gaussian noise with zero mean and variance N_0.

II. An Approximate MMSE Equalizer

The task of the receiver is to detect the transmitted symbols $\{s_n\}$ given the received observation $\{r_n\}$. From (1), we see that the desired symbol is corrupted with ISI and AWGN. An equalizer is needed to combat ISI and to improve the error rate performance. The focus of this study concerns the use of linear MMSE equalization. The equalizer coefficients are usually calculated by recursive adaptation or by direct computation based on channel estimates. If the channel is perfectly estimated and if the sequence of step sizes in the recursive algorithm is suitably chosen, the directly computed equalizer coefficients will be equal to the steady-state value of the recursively adapted coefficients [10]. In this paper, we consider the latter approach. The MMSE equalizer (with $2L + 1$ taps and detection delay d) is illustrated in Fig. 2 and is designed to minimize the mean square error (MSE) between the equalizer output z_n and symbol s_{n-d} [12]

$$\epsilon_n = \mathrm{E}\{|z_n - s_{n-d}|^2\} = \mathrm{E}\{|\mathbf{c}^* \mathbf{r}_n - s_{n-d}|^2\},$$

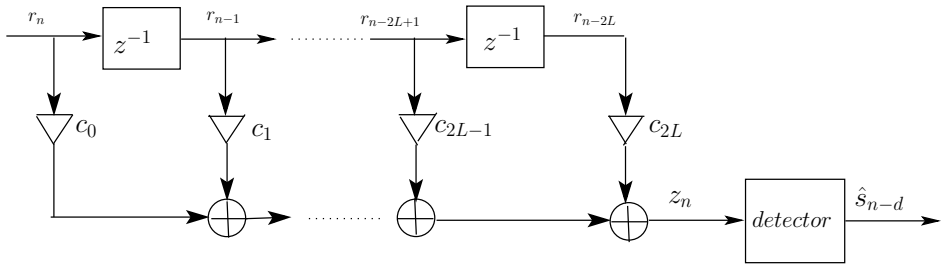

Fig. 2. MMSE equalizer with $2L+1$ taps and detection delay d.

where $\mathrm{E}(\ )$ denotes expectation (statistical averaging), and the superscript operator $(\ )^*$ is the conjugate transpose operation when applied to matrices and vectors, and simply the conjugate when applied to scalars. The output z_n is formed as

$$z_n = \sum_{k=0}^{2L} c_k^* r_{n-k} = \mathbf{c}^* \mathbf{r}_n,$$

where $\mathbf{r}_n = \begin{bmatrix} r_n & r_{n-1} & \cdots & r_{n-2L+1} & r_{n-2L} \end{bmatrix}^T$, and $\mathbf{c} = \begin{bmatrix} c_0 & c_1 & \cdots & c_{2L-1} & c_{2L} \end{bmatrix}^T$, where ^{T} stands for transpose operation. The coefficients vector is computed as

$$\mathbf{c} = (\mathrm{E}[\mathbf{r}_n \mathbf{r}_n^*])^{-1} (\mathrm{E}[\mathbf{r}_n^* s_{n-d}])^* = \mathbf{R}^{-1} \mathbf{p}^*.$$

where $\mathbf{p} = \mathrm{E}[\mathbf{r}_n^* s_{n-d}]$ is the crosscorrelation vector, and $\mathbf{R}^{-1}$ is the inverse of the autocorrelation matrix $\mathbf{R}$, which is derived as

$$\mathbf{R} = \mathrm{E}[\mathbf{r}_n \mathbf{r}_n^*] = \mathrm{E} \begin{bmatrix} r_n r_n^* & r_n r_{n-1}^* & \cdots & r_n r_{n-2L}^* \\ r_{n-1} r_n^* & r_{n-1} r_{n-1}^* & \cdots & r_{n-1} r_{n-2L}^* \\ \vdots & \cdots & \ddots & \vdots \\ r_{n-2L} r_n^* & r_{n-2L} r_{n-1}^* & \cdots & r_{n-2L} r_{n-2L}^* \end{bmatrix}.$$

Its diagonal elements are computed as

$$\begin{aligned} \mathrm{E}[r_n r_n^*] &= \mathrm{E}[r_{n-1} r_{n-1}^*] = \cdots = \mathrm{E}[r_{n-2L} r_{n-2L}^*] \\ &= \mathrm{E}[(h_0 s_n + h_1 s_{n-1} + h_2 s_{n-2} + v_n)(h_0 s_n + h_1 s_{n-1} + h_2 s_{n-2} + v_n)^*] \\ &= (\mathrm{E}[|h_0|^2] + \mathrm{E}[|h_1|^2] + \mathrm{E}[|h_1|^2]) E_s + N_0 = (P_0 + P_1 + P_2) E_s + N_0, \end{aligned}$$

where $P_i = \mathrm{E}[|h_i|^2],\ i \in \{0, 1, 2\}$ represents the average power of each path, and E_s is the average symbol energy. For non-diagonal elements, e.g., $\mathrm{E}[r_n r_{n-1}^*]$, it can be shown that

$$\mathrm{E}[r_n r_{n-1}^*] = \mathrm{E}[(h_0 s_n + h_1 s_{n-1} + h_2 s_{n-2} + v_n)(h_0 s_{n-1} + h_1 s_{n-2} + h_2 s_{n-3} + v_{n-1})^*] = 0.$$

The previous equation holds since $\mathrm{E}[h_i h_j^*] = \mathrm{E}[h_i]\,\mathrm{E}[h_j^*] = 0$, if $i \neq j$ (different paths are not correlated) and $\mathrm{E}[s_m^* s_n] = 0$, if $s_m \neq s_n$. To illustrate this point, let us reform $\mathrm{E}[s_m^* s_n]$ as

$$\mathrm{E}[s_m^* s_n] = \mathrm{E}[e^{-j\theta_m} e^{j\theta_n}] = \mathrm{E}[e^{j(\theta_n - \theta_m)}] = \mathrm{E}[e^{j\Delta\theta}],$$

where $\theta_m(\theta_n)$ is the phase of $s_m(s_n)$, and $\Delta\theta = \theta_n - \theta_m$, which takes 4 possible values $0, \frac{\pi}{2}, \pi, \frac{3\pi}{2}$ with equal probability in the case of the QPSK constellation. Thus

$$\begin{aligned}\mathrm{E}[s_m^* s_n] = \mathrm{E}[e^{j\Delta\theta}] &= P_r\{\Delta\theta = 0\}e^{j0} + P_r\{\Delta\theta = \pi/2\}e^{j\pi/2} \\ &+ P_r\{\Delta\theta = \pi\}e^{j\pi} + P_r\{\Delta\theta = 3\pi/2\}e^{j3\pi/2} \\ &= \frac{1}{4}e^{j0} + \frac{1}{4}e^{j\pi/2} + \frac{1}{4}e^{j\pi} + \frac{1}{4}e^{j3\pi/2} = 0. \end{aligned} \tag{2}$$

The same result holds for the 16-QAM constellation. The proof is similar to (2), and is not presented here. The autocorrelation matrix $\mathbf{R}$ can thus be simplified to $\mathbf{R} = [(P_0 + P_1 + P_2)E_s + N_0]\mathbf{I}_{2L+1}$, where $\mathbf{I}_{2L+1}$ is a $(2L+1) \times (2L+1)$ identity matrix.

The crosscorrelation vector $\mathbf{p}$ for the 5-tap MMSE equalizer is formed as

$$\begin{aligned}\mathbf{p} = \mathrm{E}[\mathbf{r}_n^* s_{n-d}] &= \mathrm{E}\begin{bmatrix} r_n^* s_{n-2} \\ r_{n-1}^* s_{n-2} \\ r_{n-2}^* s_{n-2} \\ r_{n-3}^* s_{n-2} \\ r_{n-4}^* s_{n-2} \end{bmatrix}^T = \mathrm{E}\begin{bmatrix} (h_0 s_n + h_1 s_{n-1} + h_2 s_{n-2} + v_n)^* s_{n-2} \\ (h_0 s_{n-1} + h_1 s_{n-2} + h_2 s_{n-3} + v_{n-1})^* s_{n-2} \\ (h_0 s_{n-2} + h_1 s_{n-3} + h_2 s_{n-4} + v_{n-2})^* s_{n-2} \\ (h_0 s_{n-3} + h_1 s_{n-4} + h_2 s_{n-5} + v_{n-3})^* s_{n-2} \\ (h_0 s_{n-4} + h_1 s_{n-5} + h_2 s_{n-6} + v_{n-4})^* s_{n-2} \end{bmatrix}^T \\ &= \begin{bmatrix} h_2^* & h_1^* & h_0^* & 0 & 0 \end{bmatrix} E_s. \end{aligned} \tag{3}$$

where the decision delay d is determined by the sum of the channel delay and equalizer delay. In the derivation of (3), we use the fact that $\mathrm{E}[s_m^* s_n] = 0$, if $s_m \neq s_n$; and $\mathrm{E}[v_{n-i}^* s_{n-2}] = \mathrm{E}[v_{n-i}^*]\,\mathrm{E}[s_{n-2}] = 0$. Since the first tap is usually the strongest tap in the FWA channels (although this may not be the case for every particular channel realization, but statistically the first tap has the largest average power), therefore there is no channel delay. For a $2L+1$ tap equalizer, the delay introduced by the equalizer is L. In the case of a 5-tap MMSE equalizer, $2L+1 = 5, d = L = 2$.

The filter coefficients vector for the 5-tap MMSE equalizer can thereby calculated as

$$\mathbf{c} = \mathbf{R}^{-1}\mathbf{p}^* = [(P_0 + P_1 + P_2)E_s + N_0]^{-1}\mathbf{I}_5\mathbf{p}^* = \frac{E_s}{N_0'}\begin{bmatrix} h_2 & h_1 & h_0 & 0 & 0 \end{bmatrix}^T, \tag{4}$$

where $N_0' = (P_0 + P_1 + P_2)E_s + N_0$. In reality, the autocorrelation matrix $\mathbf{R}$ is not restrictly diagonal for every channel realization. The equalizer coefficient vector will slightly deviate from the vector $\mathbf{c}$ derived in (4). Therefore, we called the filter derived previously an approximate MMSE (AMMSE) equalizer. The factor E_s/N_0' in (4) can be left out since it is a common scaling factor for the desired signal and ISI, as well as the noise. Therefore, it does not affect the final decision. The equalizer output can now

be formed as

$$\begin{aligned} z_n = \mathbf{c}^* \mathbf{r}_n &= \begin{bmatrix} h_2^* & h_1^* & h_0^* & 0 & 0 \end{bmatrix} \begin{bmatrix} r_n & r_{n-1} & r_{n-2} & r_{n-3} & r_{n-4} \end{bmatrix}^T \\ &= \underbrace{(|h_0|^2 + |h_1|^2 + |h_2|^2) s_{n-2}}_{\text{desired signal}} + \underbrace{h_2^* v_n + h_1^* v_{n-1} + h_0^* v_{n-2}}_{\text{noise}} \\ &\quad + \underbrace{h_2^* h_0 s_n + h_2^* h_1 s_{n-1} + h_1^* h_0 s_{n-1} + h_1^* h_2 s_{n-3} + h_0^* h_1 s_{n-3} + h_0^* h_2 s_{n-4}}_{\text{ISI}} \\ &= (|h_0|^2 + |h_1|^2 + |h_2|^2) s_{n-2} + w_n = \gamma s_{n-2} + w_n, \end{aligned} \tag{5}$$

where $\gamma = |h_0|^2 + |h_1|^2 + |h_2|^2$ is the total channel gain, and

$$w_n = h_2^* h_0 s_n + h_2^* h_1 s_{n-1} + h_1^* h_0 s_{n-1} + h_1^* h_2 s_{n-3} + h_0^* h_1 s_{n-3} + h_0^* h_2 s_{n-4} + h_2^* v_n + h_1^* v_{n-1} + h_0^* v_{n-2} \tag{6}$$

represents the combined ISI and noise. It is a complex Guassian random variable, i.e., $w_n = w_I + j w_Q \sim \mathcal{CN}(0, N_w)$, where its components $w_I \sim \mathcal{N}(0, N_w/2)$ and $w_Q \sim \mathcal{N}(0, N_w/2)$ are independent Gaussian random variables. The variance N_w can be obtained from (6) as

$$N_w = |h_2|^2(|h_0|^2 + |h_1|^2)E_s + |h_1|^2(|h_0|^2 + |h_2|^2)E_s + |h_0|^2(|h_1|^2 + |h_2|^2)E_s + (|h_0|^2 + |h_1|^2 + |h_2|^2)N_0. \tag{7}$$

A close examination of (5) reveals that the desired signal s_{n-2} available via different paths is effectively combined using the maximum ratio combining (MRC) technique. Next, we analyze the performance of the AMMSE equalizer with emphasis on the analysis of a 16-QAM modulated system. The 16-QAM constellation and maximum likelihood decision regions are depicted in Fig. 3. The decision regions can be squares (type $\mathcal{A}$), squares with one open side (type $\mathcal{B}$) or squares with two open sides (type $\mathcal{C}$). To compute the bit error probability, we first need to compute the conditional error probability for these three types of regions. Conditioned on that we send a symbol having a decision region of type $\mathcal{A}, \mathcal{B}, \mathcal{C}$, and the probabilities of making a wrong bit decision are denoted by $P_{\mathcal{A}}, P_{\mathcal{B}}, P_{\mathcal{C}}$.

To simplify the calculation, we assume that a symbol error results in a maximum of two bit errors. If the constellation is Gray coded, 1 bit error occurs when the symbol is erroneously decoded to the the symbol in non-diagonal neighbouring regions; 2 bit errors occur when the symbol is erroneously decoded to the symbol in diagonal neighbouring regions. The probability of these two events are denoted as $P_{\mathcal{A}1}, P_{\mathcal{B}1}, P_{\mathcal{C}1}$ and $P_{\mathcal{A}2}, P_{\mathcal{B}2}, P_{\mathcal{C}2}$ for symbol with decision region of type $\mathcal{A}, \mathcal{B}, \mathcal{C}$. Owing to the symmetry of the constellation, $P_{\mathcal{A}1} = P_{\mathcal{B}1} = P_{\mathcal{C}1} = \mathcal{P}_1$, and $P_{\mathcal{A}2} = P_{\mathcal{B}2} = P_{\mathcal{C}2} = \mathcal{P}_2$. Given s_{n-2} is a symbol of type $\mathcal{A}$ (e.g., the symbol $s_0 = \alpha + j\alpha$ in Fig. 3), the output of the equalizer according to (5) is $z_n = \gamma s_{n-2} + w_n = \gamma(\alpha + j\alpha) + w_I + j w_Q$. The probability $\mathcal{P}_1$ represents the conditional error probabilities

$$\begin{aligned} \mathcal{P}_1 &= P_r(\hat{s}_{n-2} = s_1 | s_{n-2} = s_0) = P_r(\hat{s}_{n-2} = s_2 | s_{n-2} = s_0) \\ &= P_r(\hat{s}_{n-2} = s_3 | s_{n-2} = s_0) = P_r(\hat{s}_{n-2} = s_4 | s_{n-2} = s_0), \end{aligned} \tag{8}$$

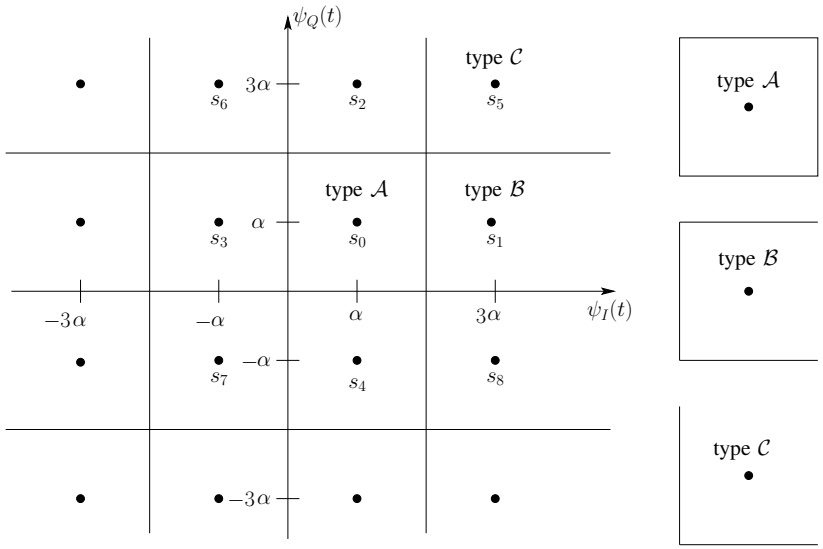

Fig. 3. 16-QAM constellation and decision regions. The minimum distance between two signal points is 2α, and $\pm\alpha, \pm 3\alpha$ are the possible amplitudes for both basis functions $\psi_I(t)$ and $\psi_Q(t)$ in the quadrature modulation. For instance, the signal $s_0(t)$ is formed as $s_0(t) = \alpha\psi_I(t) + \alpha\psi_Q(t)$. For the symbol s_0, its neighbouring symbols in the non-diagonal regions are s_1, s_2, s_3, s_4; its neighbouring symbols in the diagonal regions are s_5, s_6, s_7, s_8.

where $P_r(\hat{s}_{n-2} = s_i | s_{n-2} = s_0),\ i \in \{1, 2, 3, 4\}$ denotes the probability that the symbol s_{n-2} is erroneously decoded as s_i given s_0 is transmitted. The equalities in (8) hold since the symbol s_0 has the same distance to its non-diagonal neighbouring symbols s_1, s_2, s_3, s_4, It can be shown that

$$\begin{aligned}\mathcal{P}_1 &= P_r(\hat{s}_{n-2} = s_3 | s_{n-2} = s_0) = P_r\{\mathrm{Re}(z_n) < 0\} = P_r\{\alpha\gamma + w_I < 0\} \\ &= P_r\left\{\frac{w_I}{\sqrt{N_w/2}} < \frac{-\alpha\gamma}{\sqrt{N_w/2}}\right\} = Q\left[\frac{\alpha\gamma}{\sqrt{N_w/2}}\right], \end{aligned} \tag{9}$$

where $Q(x)$ is the complementary Gaussian cumulative distribution function [12]

$$Q(x) = \int_x^\infty \frac{1}{\sqrt{2\pi}} \exp(-t^2/2) dt = P_r\{t > x\} = P_r\{t < -x\}. \tag{10}$$

Note that the Guassian random variable t in (10) has zero mean and unit variance. Therefore, we need to normalize w_I in (9) so that $\frac{w_I}{\sqrt{N_w/2}} \sim \mathcal{N}(0, 1)$ in order that Q-function defined in (10) can be directly applied.

The probability $\mathcal{P}_2$ represents the conditional error probabilities

$$\begin{aligned}\mathcal{P}_2 &= P_r(\hat{s}_{n-2} = s_5 | s_{n-2} = s_0) = P_r(\hat{s}_{n-2} = s_6 | s_{n-2} = s_0) \\ &= P_r(\hat{s}_{n-2} = s_7 | s_{n-2} = s_0) = P_r(\hat{s}_{n-2} = s_8 | s_{n-2} = s_0). \end{aligned} \tag{11}$$

The equalities in (11) hold since the symbol s_0 has the same distance to its diagonal neighbouring symbols s_5, s_6, s_7, s_8. Using the fact that w_I and w_Q are independent Gaussian random variables, we

have

$$\begin{aligned}\mathcal{P}_2 &= P_r(\hat{s}_{n-2} = s_7 | s_{n-2} = s_0) = P_r\{\mathrm{Re}(z_n) < 0, \mathrm{Im}(z_n) < 0\} \\ &= P_r\{\alpha\gamma + w_I < 0\} \cdot P_r\{\alpha\gamma + w_Q < 0\} \\ &= P_r\left\{\frac{w_I}{\sqrt{N_w/2}} < \frac{-\alpha\gamma}{\sqrt{N_w/2}}\right\} \cdot P_r\left\{\frac{w_Q}{\sqrt{N_w/2}} < \frac{-\alpha\gamma}{\sqrt{N_w/2}}\right\} = Q^2\left[\frac{\alpha\gamma}{\sqrt{N_w/2}}\right].\end{aligned}$$

The conditional bit error probability $P_{\mathcal{A}}$ can now be computed as

$$P_{\mathcal{A}} = \frac{1}{4}[n_{\mathcal{A}1} \cdot 1 \cdot \mathcal{P}_1 + n_{\mathcal{A}2} \cdot 2 \cdot \mathcal{P}_2] = \frac{1}{4}[4\mathcal{P}_1 + 8\mathcal{P}_2] = Q\left[\frac{\alpha\gamma}{\sqrt{N_w/2}}\right] + 2Q^2\left[\frac{\alpha\gamma}{\sqrt{N_w/2}}\right],$$

where the factor $\frac{1}{4}$ is due to the fact that one 16-QAM symbol corresponds to 4 bits, and $n_{\mathcal{A}1}, n_{\mathcal{A}2}$ are the number of neighbouring regions that differ in 1 and 2 bits, respectively, from the transmitted symbol having a decision region of type $\mathcal{A}$. Similarly,

$$P_{\mathcal{B}} = \frac{1}{4}[n_{\mathcal{B}1} \cdot 1 \cdot \mathcal{P}_1 + n_{\mathcal{B}2} \cdot 2 \cdot \mathcal{P}_2] = \frac{1}{4}[3\mathcal{P}_1 + 4\mathcal{P}_2] = \frac{3}{4}Q\left[\frac{\alpha\gamma}{\sqrt{N_w/2}}\right] + Q^2\left[\frac{\alpha\gamma}{\sqrt{N_w/2}}\right];$$

$$P_{\mathcal{C}} = \frac{1}{4}[n_{\mathcal{C}1} \cdot 1 \cdot \mathcal{P}_1 + n_{\mathcal{C}2} \cdot 2 \cdot \mathcal{P}_2] = \frac{1}{4}[2\mathcal{P}_1 + 2\mathcal{P}_2] = \frac{1}{2}Q\left[\frac{\alpha\gamma}{\sqrt{N_w/2}}\right] + \frac{1}{2}Q^2\left[\frac{\alpha\gamma}{\sqrt{N_w/2}}\right],$$

where $n_{\mathcal{B}1}, n_{\mathcal{B}2}$ ($n_{\mathcal{C}1}, n_{\mathcal{C}2}$) are the number of neighbouring regions that differ in 1 and 2 bits, respectively, from the transmitted symbol having a decision region of type $\mathcal{B}$ ($\mathcal{C}$).

To simplify the notations, we denote $x = |h_0|^2, y = |h_1|^2, z = |h_2|^2$, and $\gamma = |h_0|^2 + |h_1|^2 + |h_2|^2 = x + y + z$, the bit error probability can be expressed as

$$\begin{aligned}&P_b(x,y,z) = \frac{1}{16}(n_{\mathcal{A}}P_{\mathcal{A}} + n_{\mathcal{B}}P_{\mathcal{B}} + n_{\mathcal{C}}P_{\mathcal{C}}) = \frac{1}{16}(4P_{\mathcal{A}} + 8P_{\mathcal{B}} + 4P_{\mathcal{C}}) \\ &= \frac{3}{4}Q\left(\frac{\alpha\gamma}{\sqrt{N_w/2}}\right) + \frac{9}{8}Q^2\left(\frac{\alpha\gamma}{\sqrt{N_w/2}}\right) = \frac{3}{4}Q\left(\frac{\sqrt{2}\alpha(x+y+z)}{\sqrt{N_w(x,y,z)}}\right) + \frac{9}{8}Q^2\left(\frac{\sqrt{2}\alpha(x+y+z)}{\sqrt{N_w(x,y,z)}}\right),\end{aligned} \tag{12}$$

where $N_w(x,y,z) = 4z(x+y)E_b + 4y(x+z)E_b + 4x(y+z)E_b + (x+y+z)N_0$ according to (7) (note that the relationship between average symbol energy E_s and average bit energy E_b for 16-QAM is $E_s = 4E_b$), and $n_{\mathcal{A}} = 4, n_{\mathcal{B}} = 8, n_{\mathcal{C}} = 4$ are the number of $\mathcal{A}, \mathcal{B}$, and $\mathcal{C}$ type regions, respectively, in the constellation. For the 16-QAM constellation illustrated in Fig. 3, the average symbol energy is $E_s = 4E_b = \frac{1}{16}[4(\alpha^2 + \alpha^2) + 8(\alpha^2 + 9\alpha^2) + 4(9\alpha^2 + 9\alpha^2)] = 10\alpha^2$. Therefore, we have $\alpha = \sqrt{\frac{2E_b}{5}}$, and (12) can be reformed as

$$P_b(x,y,z) = \frac{3}{4}Q\left[\sqrt{\frac{4E_b}{5N_w(x,y,z)}}\,(x+y+z)\right] + \frac{9}{8}Q^2\left[\sqrt{\frac{4E_b}{5N_w(x,y,z)}}\,(x+y+z)\right]. \tag{13}$$

Random variable x is non-central chi-square distributed with 2 degrees of freedom and probablity density function (PDF) [12]

$$p(x) = \frac{1}{2\sigma^2}\exp\left(-\frac{x+s^2}{2\sigma^2}\right)I_0\left(\frac{\sqrt{x}s}{\sigma^2}\right), \qquad x \geq 0 \tag{14}$$

where $\sigma^2 = \mathrm{var}[\mathrm{Re}(h_0)] = \mathrm{var}[\mathrm{Im}(h_0)]$ ($\mathrm{var}[x]$ denotes the variance of a random variable x), and the noncentrality parameter $s^2 = (\mathrm{Re}\{\mathrm{E}(h_0)\})^2 + (\mathrm{Im}\{\mathrm{E}(h_0)\})^2$. The operator $\mathrm{Re}(x)/\,\mathrm{Im}(x)$ denotes the real (imaginary) part of a complex variable x. Random variables y, z have central chi-square distribution with 2 degrees of freedom and PDFs

$$p(y) = \frac{1}{\gamma_1}\exp\left(-\frac{y}{\gamma_1}\right); \qquad y \geq 0$$
$$p(z) = \frac{1}{\gamma_2}\exp\left(-\frac{z}{\gamma_2}\right), \qquad z \geq 0 \tag{15}$$

where $\gamma_1 = \mathrm{E}[|h_1|^2],\ \gamma_2 = \mathrm{E}[|h_2|^2]$ stand for the average gain of the first and second path, respectively. To obtain the error probability when x, y, z are random, we must average $P_b(x, y, z)$ given in (13) over the distribution of x, y, z (given in (14), (15)), i.e.,

$$\begin{aligned}\bar{P}_b &= \int_0^\infty\int_0^\infty\int_0^\infty P_b(x,y,z)p(z)p(y)p(x)dxdydz \\ &= \frac{1}{2\sigma^2\gamma_1\gamma_2}\int_0^\infty\int_0^\infty\int_0^\infty P_b(x,y,z)\exp\left(-\frac{x+s^2}{2\sigma^2}\right)I_0\left(\frac{\sqrt{x}s}{\sigma^2}\right)\exp\left(-\frac{y}{\gamma_1}\right)\exp\left(-\frac{z}{\gamma_2}\right)dzdydx,\end{aligned} \tag{16}$$

where the expression of $P_b(x, y, z)$ is given in (13).

To conserve space, we omitted the detailed analysis for a QPSK modulated system. However, following the procedure shown in [13] for coherent detection, the average bit error probability for the AMMSE equalization can be derived similarly as

$$\begin{aligned}\bar{P}_b &= \int_0^\infty\int_0^\infty\int_0^\infty P_b(x,y,z)p(z)p(y)p(x)dxdydz \\ &= \frac{1}{2\sigma^2\gamma_1\gamma_2}\int_0^\infty\int_0^\infty\int_0^\infty Q\left[\sqrt{\frac{2E_b}{N_w(x,y,z)}}(x+y+z)\right] \\ &\quad\cdot\exp\left(-\frac{x+s^2}{2\sigma^2}\right)I_0\left(\frac{\sqrt{x}s}{\sigma^2}\right)\exp\left(-\frac{y}{\gamma_1}\right)\exp\left(-\frac{z}{\gamma_2}\right)dzdydx.\end{aligned} \tag{17}$$

The theoretical bit error probabilities calculated by (16) and (17) are compared with that produced by the simulation results in the next section to validate their accuracy.

III. Analytical Results and Performance Comparison

Comparison between analytical and simulation results is presented in this section in order to verify the theoretical analysis conducted in the previous section. The simulation results are averaged over 1000 channel realizations. During each Monte-Carlo run, the block size is set to 10000 bits, which corresponds to 5000 QPSK symbols or 2500 16-QAM symbols. The channel coefficients vary from one block to another, however, they are assumed to remain constant during the transmission of one block of data. In the simulations, we assume perfect channel state information (CSI), i.e., $\hat{\mathbf{h}} = \mathbf{h}$. The analytical curves are derived by numerical integration of the equations (16), (17) where the parameters are set to $\sigma^2 = 0.175, s^2 = 0.36$ and $\gamma_1 = 0.223,\ \gamma_2 = 0.07$.

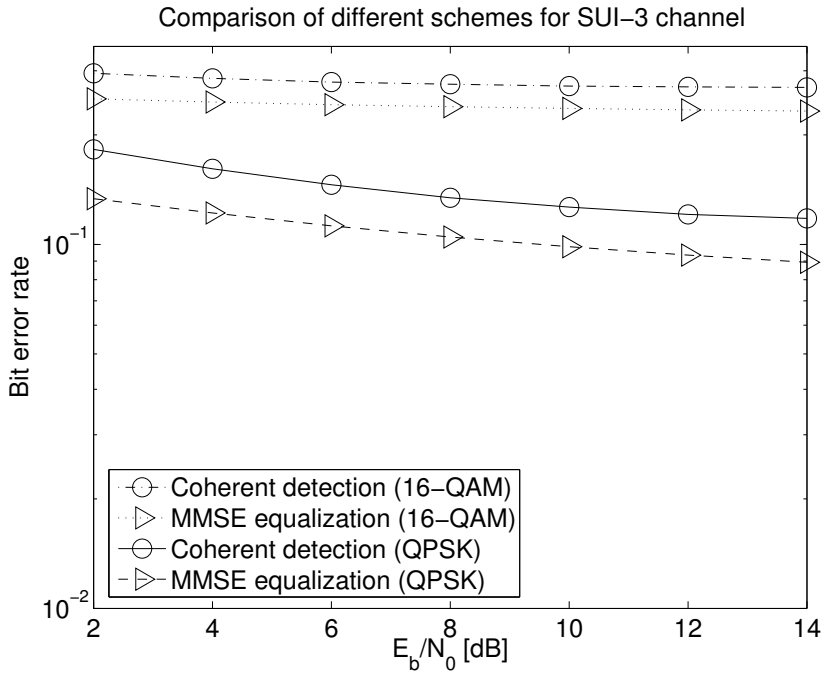

Fig. 4. Performance comparison: coherent detection vs. MMSE equalization.

In Fig. 4, we compare the performance of the MMSE equalization with that of the conventional coherent detection using results from simulation. Obviously, the linear MMSE equalizer performs better in both QPSK and 16-QAM modulated systems. The reason is simply that conventional coherent detection does not take the ISI into account, and is consequently more vulnerable to the detrimental effects of ISI. Employing equalization improves the performance, although the improvement in this context is rather limited.

The performance of the linear MMSE equalizer is further examined in Fig. 5. We observe a slight discrepancy between the theoretical analysis for 16-QAM modulation expressed by (16) and the simulation results. However, the gap becomes smaller as SNR increases. The figure also shows that the theoretical analysis for the QPSK modulated systems expressed by equation (17) is in close agreement with the simulation results for E_b/N_0 values between 4 and 6 dB. They, however, slightly deviate from each other at other SNR values. Comparing these two modulation schemes, it is evident that the QPSK modulation is more robust but supports a lower data rate, while 16-QAM supports a higher data rate but has much worse performance. It is clear to see from Fig. 5 that the SUI-3 channel is a harsh channel, and a simple MMSE equalizer is not sufficient to combat ISI.

IV. Conclusions

An approximate linear MMSE equalizer for the QPSK and 16-QAM modulated FWA systems with SUI-3 channel model is theoretically analyzed in this paper. The analysis reveals that the MMSE algorithm

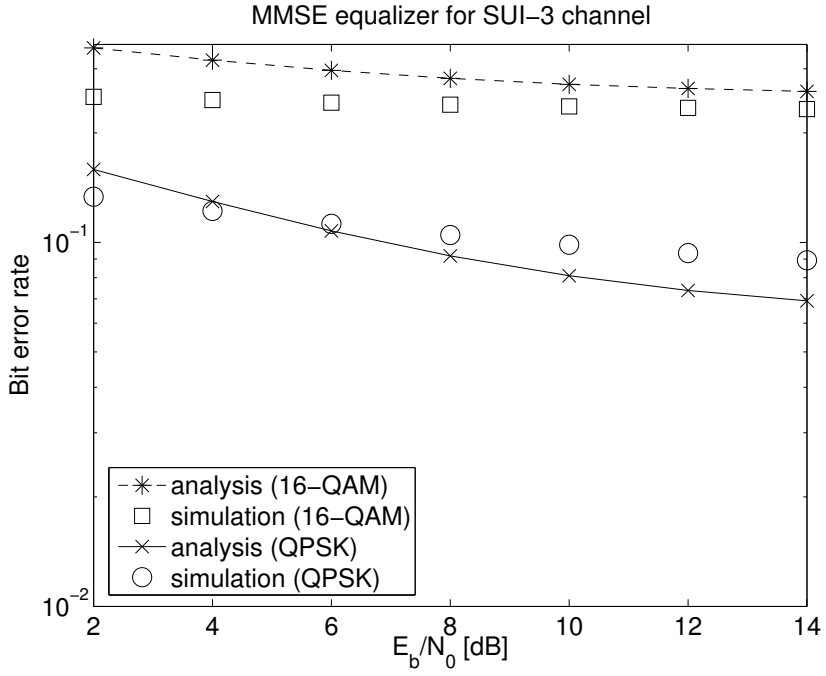

Fig. 5. Performance of 5-tap AMMSE equalizer: analysis vs. simulations.

employs an MRC technique to combine the signals from different paths. Comparison with the simulation results shows that the analysis is reasonably accurate. Both simulation and analysis indicate that the SUI-3 channel is very hostile, and consequently, traditional schemes such as linear MMSE equalization will therefore not suffice. Combined channel coding and equalization are needed to remove the detrimental effect of ISI and to improve the system performance. This will be the subject of future research by the authors.

REFERENCES

[1] H. Bolcskei. "Fixed Broadband Wireless Access: State of the Art, Challenges, and Future Directions". *IEEE Communication Magazine*, pp. 100–108, Jan. 2001.

[2] IEEE 802.16 Working Group on Broadband Wireless Access Standards. available at *http://grouper.ieee.org/groups/802/16/*. 2002.

[3] Draft ETSI TS 101, Broadband Radio Access Networks (BRAN), HIPERMAN. available at *http://portal.etsi.org/bran/Summary.asp*, 2002.

[4] I. Koffman. "Broadband fixed wireless access solutions based on OFDM access in IEEE802.16". *IEEE Communication Magazine*, vol. 40, pp. 96–103, April, 2002.

[5] E. Bartsch, I. Wassell, M. Sellars. "Equalization requirement study for broadband MMDS wireless access systems". *Proc. International Symposium on Communications*, Nov. 2001.

[6] E. Bartsch, I. Wassell. "An adaptive space-time DFE combined with successive interference cancellation". *Proc. WCNC*, vol. 2, pp. 757–761, March 2002.

[7] B. Saltzberg. "Intersymbol interference error bounds with application to ideal bandlimited signalling". *IEEE Transactions on Information Theory*, vol. 14, no. 4, pp. 563–568, July 1968.

[8] S. H. Tseng. "Optimum diversity combining and equalization over interference-limited cellular radio channel". *IEEE Transactions on Vehicular Technology*, vol. 47, no. 1, pp. 103–118, Feb. 1998.

[9] S. C. Lin. "Accurate error rate estimate using moment method for optimum diversity combining and MMSE equalisation in digital cellular mobile radio". *IEE Proceedings on Communications*, vol. 149, no. 3, pp. 157–165, June 2002.

[10] J. E. Smee, N. C. Beaulieu. "Error-rate evaluation of linear equalization and decision feedback equalization with error propagation". *IEEE Transactions on Communications*, vol. 46, no. 5, pp. 656–665, May 1998.

[11] V. Erceg. "An empirically based path loss model for wireless channels in suburban environments". *IEEE JSAC*, vol. 17, no. 7, pp. 1205–1211, July 1999.

[12] J. Proakis. *Digital Communications*, 3rd edition, McGraw-Hill, 1995.

[13] P. Xiao, R. Carrasco, I. Wassell. "Performance Analysis of Conventional Detection in BFWA Systems". In *Proc. Second IFIP International Conference on Wireless and Optical Communications Networks, WOCN'2005*, pp. 447-452, March 2005, UAE.